ELSEVIER

Polymer 40 (1999) 1441–1449

polymer

Orientation of a longitudinal polymer liquid crystal in a constant magnetic field

Witold Brostow[a,*], Elena A. Faitelson[b], Mihail G. Kamensky[b], Vadim P. Korkhov[b], Yuriy P. Rodin[b]

[a]*Departments of Materials Science and Chemistry, University of North Texas, Denton, TX 76203-5310, USA*
[b]*Institute of Polymer Mechanics of the Latvian Academy of Sciences, Aizkraukles iela 23, 1006 Riga, Latvia*

Received 2 October 1997; revised 20 March 1998; accepted 6 May 1998

Abstract

PET/0.6 PHB melt, where PET is poly(ethylene terephthalate), PHB is *p*-hydroxybenzoic acid and 0.6 is the mole fraction of the second (liquid crystal, LC) component in the copolymer, was subjected to constant magnetic fields at several temperatures in the range 240–315°C, cooled to 25°C, and then studied by x-ray diffractometry, electron diffractometry, scanning electron microscopy (SEM), dilatometry (TMA) and thermogravimetry (TGA). Given the anisotropy of the magnetic susceptibility, significant orientation effects are found. The extent of orientation was evaluated as a function of the magnetic field strength, time of the field imposition and temperature; cyclic fields were also applied. Large changes in the extent of material orientation are connected to the phase transitions determined before [9]. The LC-rich islands [4] cause channeling of flexible sequences between the LC sequences, as predicted from an extension [20] of the statistical–mechanical theory of Flory [21]. In the phase region of coexistence of the smectic E, smectic B and isotropic phases there is a growth of the size of the islands—a consequence of increased mobility. However, in the next higher temperature region, where the smectic E phase is no longer present, one observes gradual dissolution of the islands along with the temperature increase. These conclusions are derived from both x-ray diffractometry and SEM. The phase transition temperatures from TMA agree with those found by other techniques. Linear expansivity is negative along the orientation direction, but it becomes ≈ 0 after heating to 150°C. Electron diffractometry shows that the islands are elongated. TGA results show that the thermal degradation of the material in air plays a role only above 360°C. In general, the properties seem to depend on the extent of orientation but not on the nature of the field such as shear or magnetic.

Keywords: PLC orientation; Longitudinal polymer liquid crystal; Magnetic field

1. Introduction

Engineering polymers (EPs) are typically flexible, which imposes well known limitations on their mechanical performance. Better mechanical properties can be achieved by using heterogenous polymers (HCs) such as carbon-fiber reinforced plastics, or polymer liquid crystals (PLCs). HCs provide directional reinforcement; applying external forces 'the wrong way' results in fiber pullout and delamination of layer structures. Three kinds of PLCs exist: lyotropic, barotropic and thermotropic [1,2]. Lyotropics require 'exotic' highly corrosive solvents for processing. Barotropic PLCs, discovered by Hsiao et al. [3] and so named in Ref. [1] are rare. Thus, particularly interesting are the thermotropic PLCs; they can be usually processed with ordinary thermoplastics processing equipment and exhibit outstanding properties for a variety of applications.

Many properties of thermotropic PLCs are related to their ease of orientation in external fields (electric, magnetic, shearing). PLCs are typically multiphasic and contain at least one LC-rich phase which consists of *islands* [4]. The orientation occurs predominantly—but not only—in the islands, a phenomenon that we shall consider below in some detail. Effects of shearing fields and the rheology of these PLCs have been investigated reasonably extensively [5]—including our own work on EP + PLC melts [6]. Much less is known about their behavior in magnetic fields [7]—which is one of the motivations for the present work.

There exists a variety of molecular structures of PLCs, as classified by one of us [1,2,8]. The simplest are the longitudinal PLCs, with the LC sequences in the main chain and oriented along the polymer backbone. Following the rule 'first things first', the PLC chosen for this study belongs to this category.

* Corresponding author.

0032-3861/98/$ - see front matter
PII: S0032-3861(98)00357-7

2. Experimental

PET/0.6 PHB, where PET is poly(ethylene terephthalate), PHB is *p*-hydroxybenzoic acid and 0.6 is the mole fraction of the second (LC) component in the copolymer, is the same as used in our earlier investigations [4,6,9–12]. Its detailed characteristics have been provided in Ref. [9] including the phase diagram of PET/*x*PHB copolymers as a function of the mole fraction *x* obtained from 18 laboratories worldwide. Upon melting at 200°C our PET/0.6PHB consists of a smectic E and the isotropic phase. Around 230°C a smectic B phase appears in addition to the other two phases. Around 330°C there is another phase transition at which the smectic E phase disappears. Finally at $\approx$ 420°C we have an also reproducible clearing temperature. Thus, our samples are thermally stable at high temperatures, an important advantage of PLCs in general in comparison to EPs and other flexible polymers. The phase diagram constructed in Ref. [9] is in this respect also confirmed by the TGA results in the air atmosphere reported in Section 4 below.

Granulated copolymer was dried under vacuum at 110°C for 20 h, then heated in a Teflon crucible up to 280°C, the resulting melt kneaded thoroughly for 1 h, and finally slowly cooled to room temperature.

An electric oven was placed between pole tips of a constant electromagnet. Each specimen was heated to a desired temperature *T* and kept there for 1.5 h before magnetic treatment. *T*, magnetic induction *B* and time *t* were varied one at a time. After the treatment the oven was switched off but the magnetic field maintained during cooling to 25°C.

We have also studied effects of cyclic field imposition upon orientation. Two regimes were applied for that purpose. The first regime consisted of five stages. One started with a heating–field imposition–cooling cycle as described above. In the second stage the specimen was heated up to the same temperature as in the first cycle, held for 1 h at that temperature without the magnetic field, and then cooled down. The third and fifth stages were identical to the first one, while the fourth stage was the same as the second. Thus, the repetition of high temperature treatment made possible eliminating effects of the thermal history of the sample; at the same time, the presence and absence of the magnetic field made possible separation of effects of that field from the effects of temperature changes. X-ray diffractometry was performed after each cycle.

In the second regime there were also five stages, with the field switched on and off in the same way. However, a constant temperature was maintained without cooling, except after the fifth stage. The diffractometry was performed only once after the fifth stage.

We have used the DRON-3M diffractometer supplied by Burevestnik, St. Petersburg, Russia, with Cu K_α and Ni K_α radiation. The x-ray scattering intensity as a function of the diffraction angle θ was determined in directions parallel and perpendicular to the magnetic field force lines in the specimens. The scanning step of the x-ray patterns was 1°. Diffraction maxima were scanned with a step of 0.05°. The time of impulse collection at each step was 30 s. The error in the peak location was less then 0.025°, and the error in scattering intensities $< 0.1\%$.

Linear isobaric expansivity was determined by the thermomechanical analysis (TMA) method using the UIP-70 M apparatus from TsKB Unikalnye Aparaty, Moscow, Russia. The constant heating rate amounted to 1.25 K/min. The specimen deformation was determined with a capacitor transducer which provided length determination with an accuracy of $\pm 5 \times 10^{-3}$ mm.

The polymer surfaces were studied with scanning electron microscopy (SEM) using the MREM-100 microscope from TsKB Unikalnye Aparaty, Czernogolovka, Russia. The surfaces were first polished and etched in a plasma in a corona discharge for 30 min. To prevent overheating of

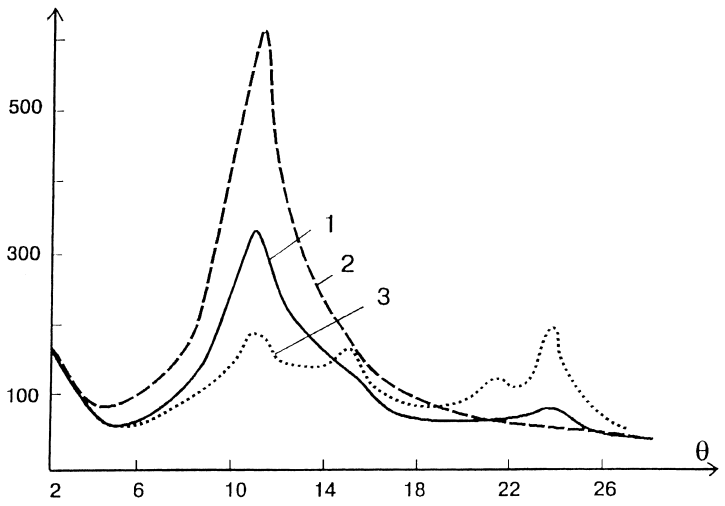

Fig. 1. Dimensionless scattering intensity *I* as a function of the diffraction angle θ obtained with Cu K_α radiation for PET/0.6PHB with the $B = 0.65$ Tesla field at 300°C. Explanations in the text.

the specimens, the following regime was applied: etching for 1 min, cooling for 15 min, etching again, and so on until the required total etching time was accumulated. After etching the surface was covered with silver by sputtering.

Thermogravimetric analysis (TGA) was performed with the Q-1500D derivatograph from MOM, Budapest, Hungary. The constant heating rate was 4 K/min.

Electronography was performed using the EF-4 device from Carl Zeiss, Jena, Germany, in the reflection mode. The accelerating voltage was 50 kV.

3. X-ray diffractometry

In Fig. 1 we show the dimensionless scattering intensity I as a function of the diffraction angle θ obtained with the Ni K_α radiation from specimens treated for 45 min with $B =$ 0.65 Tesla field at 300°C. Curve 1 corresponds to the relatively unoriented sample obtained from the kneading described at the beginning of the previous section. Curve 2 represents the oriented sample placed perpendicular to the field force lines direction, curve 3 for the sample oriented parallel to the lines.

In curve 1 we see two fairly diffuse maxima at $\theta = 10.8°$ and 23.65°. The former represents intermolecular diffraction; it has been known for decades that such a peak shows up as the only one in unoriented flexible polymers [13]. The second peak, absent in flexible polymers, is known to be characteristic for PLCs [14–16], hence it has to be related to the existence of the PLC-rich islands. Research groups investigating orientation in PLCs [14,15] confine themselves to qualitative arguments. An exception is an attempt by Tsukruk and coworkers to use parameters defined for flexible coils to represent LC orientation [16]. This attempt has not been recognized as plausible, so that 6 years later, Allgaier and Finkelmann, who studied both magnetic properties and x-ray diffractometry of a comb PLC [17], considered the anisotropy of their PLC qualitatively only. This situation behooves us to formulate a quantity based on diffractometry of solids which can represent the extent of orientation. Given the absence of that second and further peaks in flexible polymers, we define the following relative measure of orientation in PLCs

$$d_{\text{orient}} = \frac{\text{(the largest non−first maximum intensity)}}{\text{(the first maximum intensity)}} \qquad (1)$$

Our degree of orientation d_{orient} embraces both the effects of 'natural' ordering (different directions in different islands) present without the field and the orientation imposed by the field. d_{orient} should not be confused with the Hermans order parameter s which has been in use for decades and is defined for instance in Ref. [18]; s varies in the range between $-1/2$ and $+1$. In the following we always use the diffraction angle $\theta = 23.65°$ for the evaluation of the numerator and $\theta = 10.8°$ for the denominator in Eq. (1). For our relatively unoriented sample represented by the curve 1 in Fig. 1 we have $d_{\text{orient}} =$ 0.16.

Curve 2 in Fig. 1 exhibits a fairly strong but somewhat diffuse maximum at $\theta = 10.9°$, a slightly larger angle than for the analogous maximum in Curve 1. Apparently, the ordering which takes place going from sample 1 to sample 2 results in the shortening of the average intersegmental distances—as in fact is expected. We remember that curve 2 corresponds to the perpendicular direction of the field lines with respect to the material orientation and the x-ray pattern is equatorial.

Curve 3, meridional, exhibits four clear diffuse maxima, located approximately at the diffraction angles $\theta =$ 11.0, 14.9, 21.4 and 23.65°. These values agree with those obtained by previous investigators for the same copolymer [19]. There seems to be an extra maximum at $\theta \approx 3.5°$ but the intensity at that angle is low. There is also a shoulder at $\theta \approx 13.5°$ which is hard to separate from the adjacent large peak at $\theta = 14.9°$. The scattering intensity at $\theta \approx 11.0°$ is much lower than for curve 1, which means the interactions of the unoriented (flexible) segments are much weaker here. The other three maxima at $\theta = 14.9°$, 21.4° and 23.65° show significant effects of the orientation. For the fourth maximum from Eq. (1) we have $d_{\text{orient}} = 1.18$, more than sevenfold the value for the sample with low extent of orientation in curve 1. This difference in the values of d_{orient} testifies also to the physical significance of Eq. (1) and its utility in quantifying the effects of imposition of the magnetic field.

The time $t_{\text{equil}}(T,B)$ until an equilibrium state is reached after the imposition of a magnetic field is of interest. To elucidate this, we have measured the orientation parameter as defined by Eq. (1) as a function of time t. The results are shown in Fig. 2 for $T = 280$°C and $B = 0.65$ Tesla. We find that for this pair of T and B values we have $t_{\text{equil}}(T,B) \approx$ 25 min.

We have also investigated the orientation parameter d_{orient} as a function of the magnetic induction B. Given the results shown in Fig. 2, x-ray patterns were determined 25 min after the field imposition. The results for $T = 280$°C are shown in Fig. 3. The upper limit of B imposed was determined by the

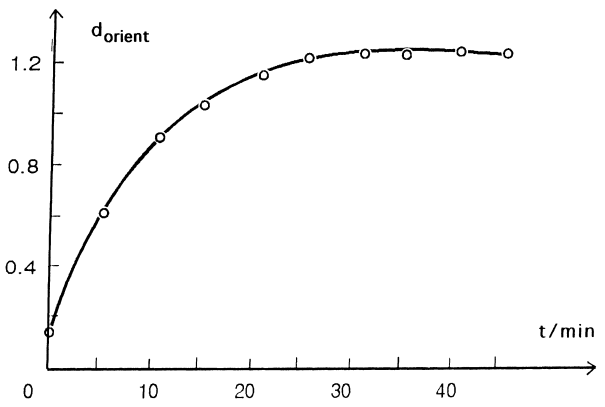

Fig. 2. The orientation parameter d_{orient} defined by Eq. (1) as a function of the time of imposition of the 0.65 Tesla magnetic field at 280°C.

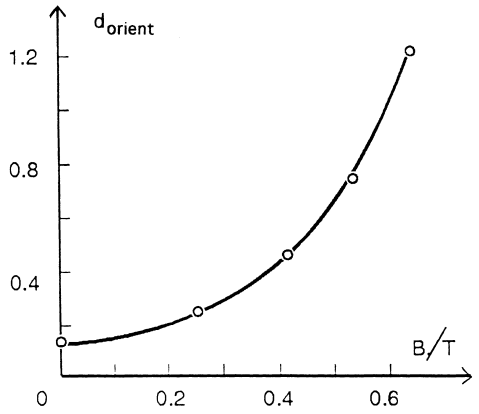

Fig. 3. The orientation parameter d_{orient} as a function of the field strength at 280°C and $t_{equil} = 25$ min.

capabilities of our equipment. One expects that at a sufficiently high field strength a saturation value of d_{orient} is achieved, but we have not reached that value.

In turn, we have studied d_{orient} as a function of temperature, again for $B = 0.65$ Tesla and $t_{equil} = 25$ min. The results are shown in Fig. 4. To interpret them, we turn to the phase diagram of PET/*x*PHB copolymers established on the basis of the results of 18 laboratories [9] already mentioned in Section 2. In the figure, we see a rapid increase in d_{orient} above 240°C. In the phase diagram we find that this is the transition temperature from region X where the phases present are smectic E (originating from PHB) and the isotropic liquid (originating from the PET constituent) to region XI where we have the coexistence of smectic E and smectic B phases along with the isotropic liquid. Thus, the creation of the second LC phase strongly increases the orientation.

At least two effects contribute to that increase. First, the presence of the smectic B phase apparently increases *channeling* and subsequent orientation of flexible PET sequences between the LC sequences. The channeling effect has been predicted by us [20] on the basis of an extension of the statistical–mechanical theory of PLCs developed by Flory [21–23] and continued by his collaborators [18,20,24].

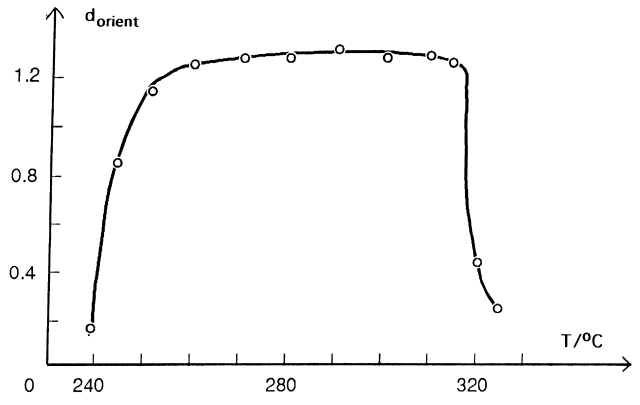

Fig. 4. The orientation parameter d_{orient} as a function of temperature for $B =$ 0.65 Tesla and $t_{equil} = 25$ min.

The other effect is related to the island size. According to Shiwaku and coworkers [19], there is little change in the island size between 120°C and the melting temperature T_m of the copolymer; they explain it in the obvious way that large-distance translational diffusion is difficult. However, at higher temperatures they observe a significant growth in the island size, as documented by their SEMicrographs at 250°C and 290°C. We note that both their temperatures are inside the Region XI—where we see such high values of d_{orient} in Fig. 4. We shall deal with this issue again in Section 5 below on the basis of our own SEM results.

Given the significance of the PHB sequences rigidity, it is worthwhile to inquire about their structure. Blackwell et al. [15] have studied that structure using x-ray as well as electron diffractometry. They have inferred that the poly-PHB chain has a stiff extended 2_1 helical conformation, with two segments (monomer units) repeating in 1.24 ± 0.02 nm.

The fall of d_{orient} above 320°C also needs to be explained. Again the phase diagram, Fig. 10 in Ref. [9], provides the answer. Around that temperature, we cross the border from region XI to region XII; in the latter we have the smectic B phase coexisting with the isotropic liquid. Apparently in that region there is enough of the isotropic phase to lower significantly the extent of orientation. The increasing amounts of thermal energy also help the destruction of orientation; we see how the lowering of orientation goes symbatically with the temperature increase.

At lower temperatures we observed the growth of the islands. We infer than at $T > 320$°C the islands undergo gradual dissolution in the PET-rich phase. An earlier wide angle x-ray scattering (WAXS) study [25] has shown that the islands contain PHB-rich crystallites. Since high anisotropy of diamagnetic susceptibility resides in the islands, the island disappearance lowers the channeling effect. Thus, it is not the rigidity of the crystallites or the individual PHB sequences which is the main creator of orientation. *The channeling effect is caused by the islands*. We note that, depending on the amount of previous processing and/or solid state mechanical deformation, the islands can be approximately spherical, ellipsoidal, or even fiber-like. We recall the solid-state orientation of PET/0.3PHB by drawing which resulted in fourfold enhancement of the elastic modulus and tensile strength [9].

The experiments reported in this paper have been performed in Riga. As noted above, the phase diagram has been put together in Denton on the basis of results obtained at a number of laboratories. Yet the transitions visible in Fig. 4 occur at the same temperatures as those delineated on the phase diagram in Ref. [9]. It is gratifying to see the agreement in pinpointing these transitions not only by different techniques but also at different locations.

In Section 2 we have defined two regimes of cyclic field imposition. Some meridional x-ray patterns obtained with Cu K_α radiation by applying these regimes are shown in Fig. 5. In both cases we had $T = 280$°C, $B = 0.65$ Tesla and $t = 25$ min. Curves 1–5 pertain to the first, curve 6 to

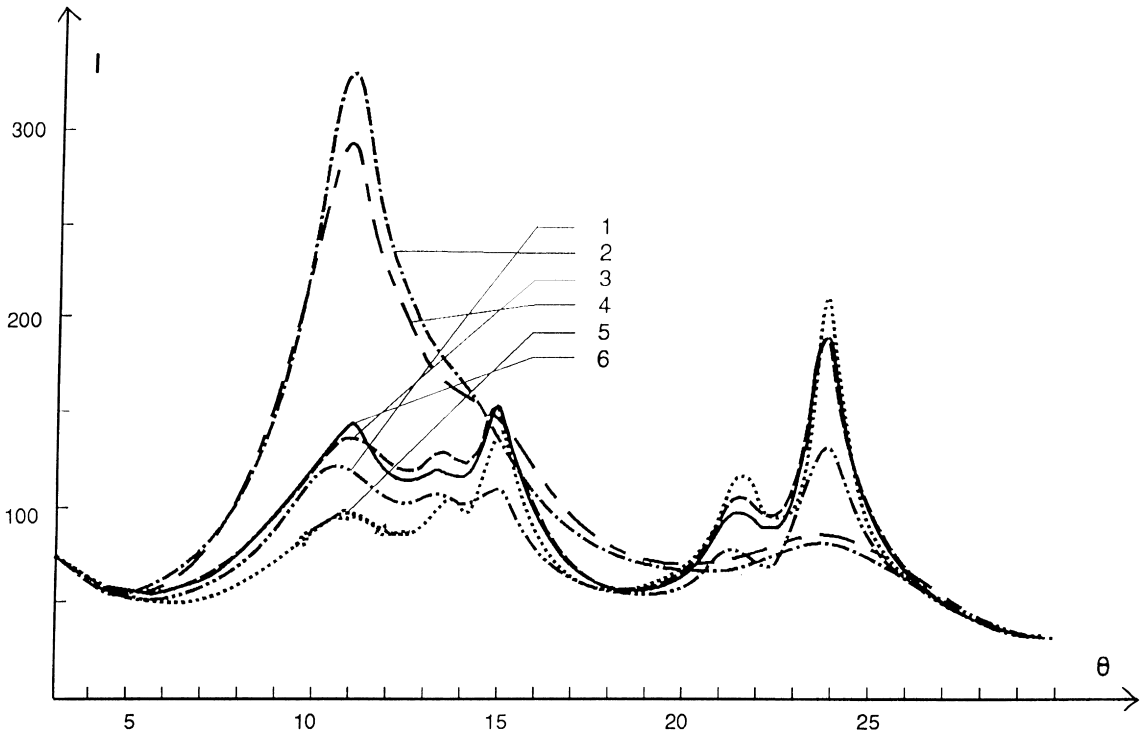

Fig. 5. Meridional scattering intensity I as a function of the diffraction angle θ obtained with Cu K_α radiation of materials subjected to cyclic magnetic fields. Explanations in the text.

the second regime. The consecutive field imposition stages (curves 1, 3 and 5) show decreases of the first maximum and increases of the other maxima. The respective values of d_{orient} for these three curves are 1.32, 2.22 and 3.45. Keeping the material at 280°C without the magnetic field largely destroys the orientation; the extent of orientation for curve 2 is the same as for curve 4, namely $d_{\text{orient}} = 0.16$. This conclusion is similar to that reached from Fig. 4 for $T > 320$°C in the presence of the magnetic field.

We recall that in the second regime the temperature was maintained constant while the field was switched on and off. Curve 6 corresponds to $d_{\text{orient}} = 1.56$ after five stages defined above. This value is higher than 1.32 from the first stage in regime 1, showing a certain accumulation of orientation in stages 1, 3 and 5. At the same time, this accumulation is distinctly lower than $d_{\text{orient}} = 3.45$ also achieved after the fifth stage but with intermittent cooling.

We have also investigated the effects of increasing the number of stages beyond five in both regimes. The changes were insignificant; apparently in both regimes, the fifth stage produced as much orientation as was possible under a given regime.

A temperature of 280°C is in the middle of the high orientation region seen in Fig. 4. We have explained that diagram in terms of the growth in size of the islands followed by their gradual dissolution at higher temperatures. The increase in d_{orient} between the first, third and fifth stages in the first regime can be explained in similar terms. Apparently the islands formed at stage 1 were only partly weakened or destroyed at stage 2; hence at stage 3 larger islands were formed, resulting in a further increase in orientation. The changes in the sequence of stages 3–4–5 were similar, and so after the fifth stage in the first regime the highest orientation was achieved. Stages beyond the fifth did not change anything because there exists a *maximum island size* for a given temperature.

We have mentioned before an earlier investigation of the same copolymer by WAXS, performed at DESY, Hamburg, in connection with the hierarchical structures of the PLCs [25]. It was found then that the islands contain crystallites, with the diameter of a single crystallite $L \approx 12$ nm. This can be contrasted with the size of the islands already known from earlier work [4] to be of the order of 1 μm. The classical formula [26] for the crystallite diameter is

$$L = k \cdot \lambda / (\theta_{1/2} \cdot \cos\theta) \tag{2}$$

where k is a constant of the order of unity, λ the x-ray wavelength and $\theta_{1/2}$ the half-width of the principal peak. Applying Eq. (2) to results for the sample represented by curve 5 in Fig. 5, we find $L \approx 10$ nm. Thus, there is a satisfactory agreement between the Hamburg and the Riga results.

4. Thermogravimetry

TGA analysis was made to see the effects—if any—of thermal degradation of the material on our results. The weight loss curve determined in the air atmosphere is

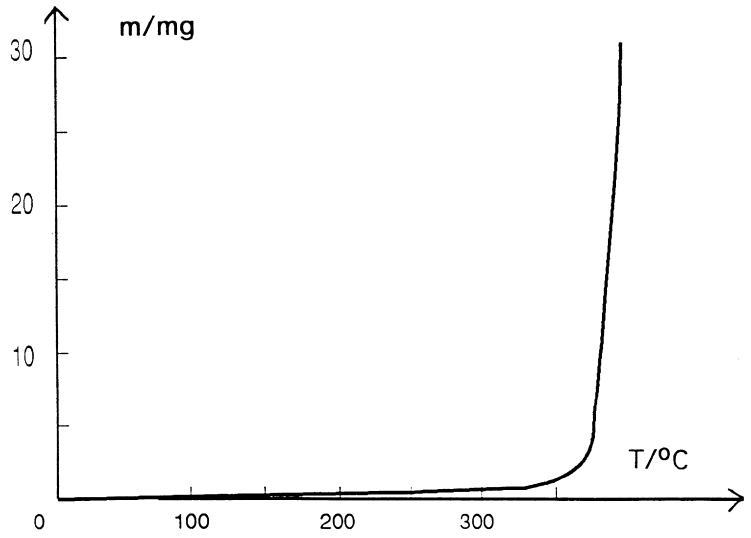

Fig. 6. Dependence of the weight loss on temperature determined by TGA in the air atmosphere. The original sample mass was 210.7 g, the constant heating rate 4 K/min.

shown in Fig. 6. We see that the thermal degradation effects appear only at temperatures exceeding 360°C or so.

5. Scanning electron microscopy

Among others, we have discussed above the size of the islands on the basis of indirect evidence from our orientation parameter d_{orient}. It was interesting to find out whether the SEM technique will provide a confirmation of these conclusions.

In Fig. 7a, we show a SEMicrograph of a little oriented sample corresponding to the x-ray diffraction pattern in Fig. 1, curve 1. While one sees indications of a two-phase structure, delineating the LC-rich islands would be difficult. Fig. 7b shows the material after one-stage application of the 0.65 Tesla magnetic field at 280°C for 5 min; the islands are more clearly visible than before. Keeping the material at the same temperature for 1 h results in the islands becoming larger and also with more distinct borders to their surroundings (Fig. 7c). It should be noted that, given the connectedness of PET and PHB sequences in the copolymer chains, very sharp island borders are not to be expected.

We have also subjected our specimens to the full five-stage regime of the first kind. The resulting structure after all five stages is shown in the micrograph in Fig. 7d. The islands are quite large and easily visible. This confirms the earlier observations of Shiwaku and coworkers [19]. More importantly, the SEM results lead to the same conclusions as already derived from x-ray diffractometry on the basis of variations of the d_{orient} parameter.

We have concluded in the preceding Section that the second cyclic regime (keeping a constant high temperature without periodical cooling) produces less orientation, apparently because of smaller islands. This conclusion is confirmed by the micrograph shown as Fig. 7e. Not only are the islands smaller than in Fig. 7d, but also their borders are less sharp.

6. Isobaric expansivity

The TMA technique provides values of linear isobaric expansivity α_{L} (also known as the 'thermal expansion coefficient'). For isotropic systems, one such determination is sufficient for the calculation of the volumetric isobaric expansivity. For anisotropic systems—such as our PLC—values of the expansivity along the three Cartesian coordinates (along the flow $\alpha_{\text{L}\|}$ and in the two directions orthogonal to the flow $\alpha_{\text{L}\perp}$) are needed for the calculation of α. Industry is becoming more and more interested in materials with low expansivities, both linear and volumetric. Because of their rigidity, PLCs have typically lower expansivities than flexible EPs.

We represent our results in the form of percentage length variation $\Delta l/l$, where l is the sample length, as a function of temperature changes in heating and cooling cycles. In Fig. 8a, we show dilatometry results for a relatively unoriented sample, whose x-ray patterns are shown in Fig. 1, curve 1. Numbers I and II pertain to the consecutive heating and cooling cycles. We observe a region with nearly constant expansivity centered approximately around 150°C. Consulting once again the phase diagram [9], we find that we are at the glass transition of the PHB constituent of the PLC.

We have also performed TMA for samples first kept at $B = 0.65$ Tesla and $T = 300$°C for 45 min and then cooled down. Fig. 8b shows the results for the sample placed in the TMA apparatus perpendicularly ($\alpha_{\text{L}\perp}$) and Fig. 8c parallel ($\alpha_{\text{L}\|}$) to the orientation direction. We see again that the

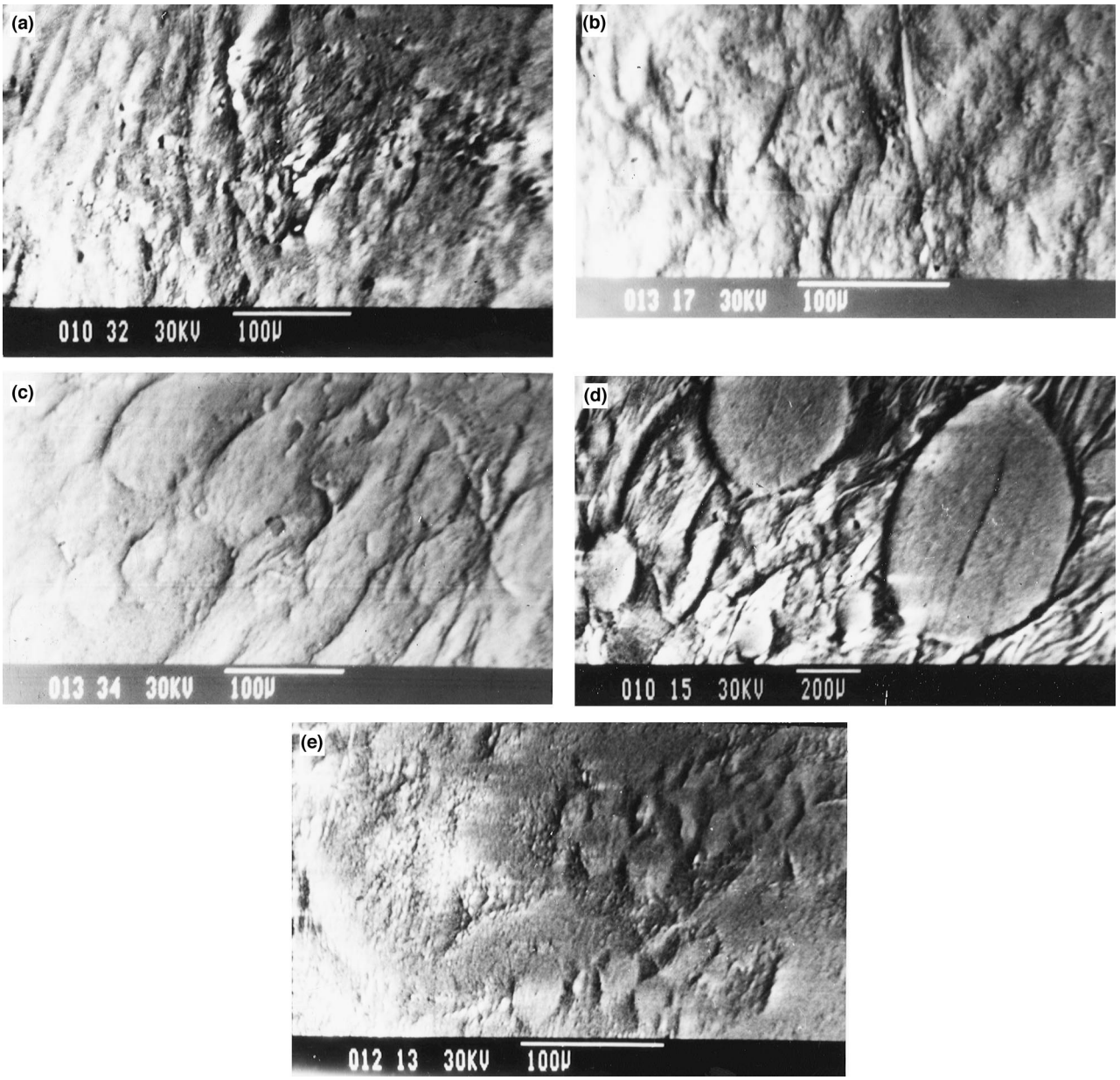

Fig. 7. Scanning electron micrographs for samples subjected to different magnetic and thermal treatment. Explanations in the text.

history of the sample—including its magnetic history—is largely erased on heating. The second heating + cooling cycle produces a much smaller difference between expansivities on heating and on cooling at a given temperature. In both Fig. 8b and Fig. 8c, the imposition of the field has accentuated the transition around 62°C, which we know [9] is the glass transition of the PET component.

Since low or negative expansivities are of high practical interest, we need to explain in particular the results in Fig. 8c. One explanation is the rubber-elastic contraction of the oriented material along the orientation direction [27,28]. This applies not only to PLCs but also to other anisotropic polymers which underwent orientation. Interestingly, the volumetric expansivity typically is positive, since the two perpendicular linear expansivities $\alpha_{L\perp}$ have larger absolute values than the absolute value of the parallel linear expansivity $\alpha_{L||}$ [28].

The explanation of $\alpha_{L||} < 0$ in terms of orientation is confirmed and perhaps amplified by our results. We recall that at 300°C as well as during subsequent cooling of the oriented sample the magnetic field was maintained. Apparently, 'attacked' by the magnetic field, the material 'defended itself' against orientation because of the entanglements acting similarly as rubber-elastic junctions and the resistance against volume change (which is so evident in elastomeric materials). Upon achieving room temperature, the field was removed and the α determination started. In the first cycle in the temperature range 44–56°C we have the

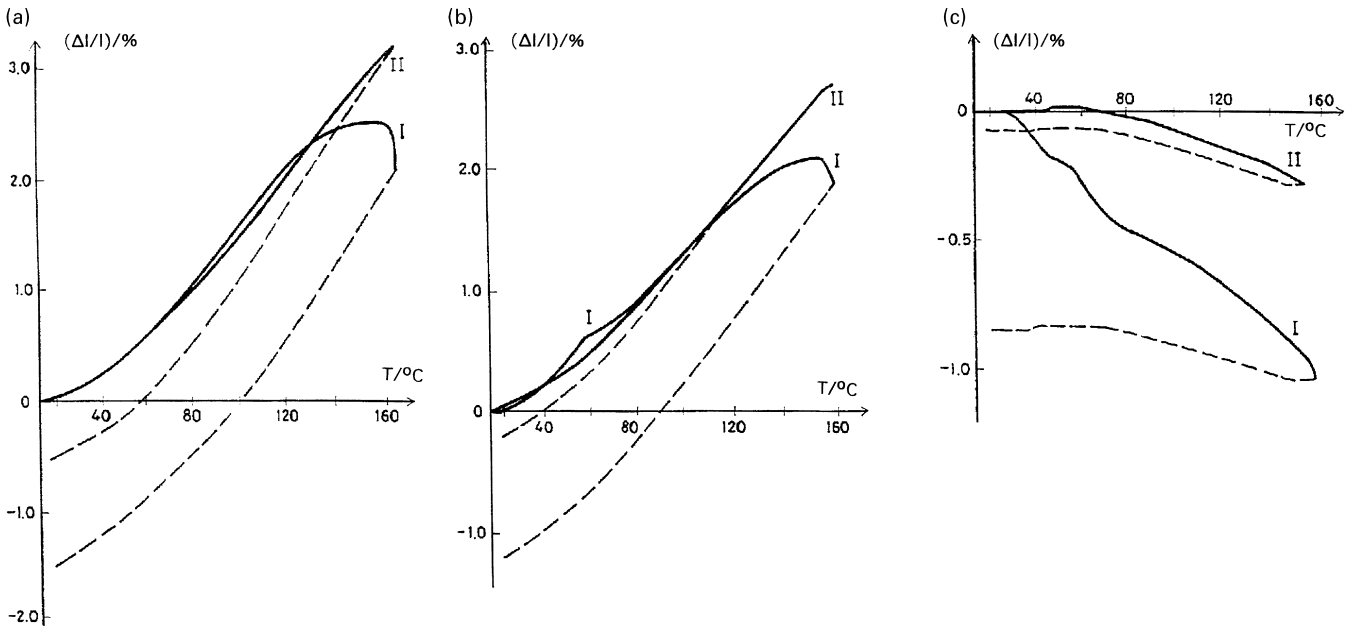

Fig. 8. Dilatometric TMA results expressed as the fractional length change $\Delta l/l$. Explanations in the text.

average for the specimens oriented parallel to the field force lines $\alpha_{L||} = -5.1 \times 10^{-5}\,K^{-1}$. Heating in the absence of the field resulted in what we call 'defense', shrinking as an attempt by the specimens to restore the pre-field structure. Whatever contraction was supposed to occur did occur during that heating stage. The maximum temperature in the first no-field cycle was 150°C, and during the cycle the material underwent relaxation towards equilibrium. We infer this because in the second cycle in a largely overlapping range 47–63°C we have $\alpha_{L||} = 0$. Apparently, there was enough orientation left in the material to assure zero expansivity.

Fig. 9. The electron diffraction pattern for the specimen subjected to cyclic magnetic fields according to regime 1 defined in Section 2.

7. Electron diffractometry

In Fig. 9, we display the results for one specimen only, corresponding to curve 5 in Fig. 5. The diffraction patterns exhibit sharp reflexes, demonstrating three-dimensional ordering in the material. We recall that there is a wide maximum in the equatorial scattering intensity diagram in Fig. 1. We infer that the crystallites in the direction perpendicular to the macromolecular orientation have small sizes, or are needle-shaped. The large crystallite axis coincides with the direction of macromolecular orientation. The islands are elongated, but not needle-shaped like the crystallites.

In conjunction with the earlier viscosity investigation in shearing fields [6], we infer that the nature of the field (tensile, shearing, magnetic) hardly affects the consequences of the orientation process. The properties depend on the extent of orientation.

Acknowledgements

Partial financial support for this work was provided by the Robert A. Welch Foundation, Houston (Grant # B-1203), by the North Atlantic Treaty Organization, Brussels (Award # LG.931044) and also by the Latvian Council of Science, Riga (Grant # 96.0683). Thanks for discussions are due to: Józef Garbarczyk at the Poznan University of Technology; Michael Hess at the Gerhard Mercator University of Duisburg; Josef Kubát at the Chalmers University of Technology, Gothenburg; Robert Maksimov at the Institute of Polymer Mechanics in Riga; and Janusz Walasek at the Technical University of Radom.

References

[1] Brostow W. Polymer 1990;31:979.
[2] Brostow W. In: Mark JE, editor. Physical properties of polymers handbook. Woodbury, NY: American Institute of Physics Press, 1996, Ch. 33.
[3] Hsiao BS, Shaw MT, Samulski ET. Macromolecules 1988;21:543.
[4] Brostow W, Dziemianowicz TS, Romanski J, Werber W. Polym Eng Sci 1988;28:785.
[5] Acierno D, Collyer AA, editors. Polymer liquid crystals—2—Rheological properties and processing. London: Chapman and Hall, 1996.
[6] Brostow W, Sterzynski T, Triouleyre S. Polymer 1996;37:1561.
[7] Brostow W, Collyer AA, editors. Polymer liquid crystals—4—Electrical, magnetic and optical properties. London: Chapman and Hall, 1999.
[8] Brostow W. Kunststoffe 1988;78:411.
[9] Brostow W, Hess M, López BL. Macromolecules 1994;27:2262.
[10] Carius H-E, Schönhals A, Guigner D, Sterzynski T, Brostow W. Macromolecules 1996;29:5017.
[11] Brostow W, Hess M, López BL, Sterzynski T. Polymer 1996;37:1551.
[12] Berry JM, Brostow W, Hess M, Jacobs EG. Polymer 1998;39:4081.
[13] Martinov MA, Vilegzhanina KA. Rentgenografia polimerov. Moscow: Nauka, 1972:124.
[14] Mitchell GR, Windle AH. Polymer 1983;24:1513.
[15] Blackwell J, Lieser G, Gutierrez GA. Macromolecules 1983;16:1418.
[16] Tsukruk VV, Shilov VV, Yenihen D. Vysokomol Soed A 1988;30:2202.
[17] Allgaier J, Finkelmann H. Macromol Chem Phys 1994;195:1017.
[18] Brostow W, Walasek J. J Chem Phys 1996;105:4367.
[19] Shiwaku T, Nakai A, Hasegawa H, Hashimoto T. Macromolecules 1990;23:1590.
[20] Blonski S, Brostow W, Jonah DA, Hess M. Macromolecules 1993;26:84.
[21] Flory PJ. Proc R Soc A 1956;234:60,73.
[22] Flory PJ, Abe A. Macromolecules 1978;11:1119.
[23] Matheson RR Jr. Flory PJ. Macromolecules 1981;14:954.
[24] Matheson RR Jr. Macromolecules 1986;19:1286.
[25] Brostow W, Hess M. Mater Res Soc Symp 1992;255:57.
[26] Kitaigorodskii AI. Rentgenostrukturnyi analiz Moscow: Nauka, 1950:650.
[27] Maswood S. Proc Ann Tech Conf Soc Plast Eng 1996;54:3614; Private communication from N.A.D. Souza, University of North Texas, 1996.
[28] Singh RP. In: Brostow W, editor. Polymer liquid crystals—3—Mechanical and thermophysical properties. London: Chapman and Hall, 1998, Ch. 8.